Transactions of NAMP 21, (2025) 41-54

Transactions of
The Nigerian Association of
Mathematical Physics
Journal homepage: https://nampjournals.org.ng

A FRACTIONAL MATHEMATICAL MODEL FOR THE DYNAMICS OF MALARIA TRANSMISSION AND CONTROL

[1,2]Daniel Omeje, [1,2] Bolarinwa Bolaji, [1,2]William Atokolo, 3Joseph Egbemhenghe
[1,2]Emmanuel Abah, [1,2]Jeremiah Amos.

[1] *Department of Mathematical Sciences, Prince Abubakar Audu University, Anyigba, Nigeria*
[2] *Laboratory of Mathematical Epidemiology, Prince Abubakar Audu University, Anyigba.*
3 *Department of Mathematics Education, Prince Abubakar Audu University, Anyigba*
(Formerly known as Kogi State University Anyigba), Nigeria

ARTICLE INFO

Article history:
Received xxxxx
Revised xxxxx
Accepted xxxxx
Available online xxxxx

Keywords:
Malaria,
Fractional,
Simulation,
Adams–
Bashforth–
Moulton.

ABSTRACT

This study examines many epidemiological features of malaria infection using a fractional-order mathematical model to assess how therapy affects the dynamics of malaria transmission. Fractional Adams–Bashforth–Moulton numerical simulations show how fractional-order values and model parameters affect malaria dynamics and control. More surface and contour plot simulations show that the prevalence of malaria would rise with increasing contact rates and less effective treatment. Additionally, the study reveals that improving treatment approaches can dramatically lower the frequency of malaria in the general population.

1.0 Introduction

Malaria is a life-threatening disease primarily found in tropical countries. It is both preventable and curable. However, without prompt diagnosis and effective treatment, a case of uncomplicated malaria can progress to a severe form of the disease, which is often fatal without treatment. It is not contagious and cannot spread from one person to another the disease is transmitted through the bites of female *Anopheles* mosquitoes. Five species of parasites can cause malaria in humans and 2 of these species – *Plasmodium falciparum* and *Plasmodium vivax* – pose the greatest threat. There are over 400 different species of *Anopheles* mosquitoes and around 40, known as vector species, can transmit the disease [1].

*Corresponding author: William Atokolo
E-mail address: williamsatokolo@gmail.com
https://doi.org/10.60787/tnamp.v21.472

Malaria symptoms usually start to show up 10–15 days following the infective insect bite. On the other hand, symptoms may not appear for up to a year in certain situations. Depending on the type of Plasmodium parasite causing the infection, the symptoms can vary, but frequent ones include: fever, chills, sweats, headaches, and aches in the muscle's exhaustion, nausea, and vomiting [2]. In Nigeria, Malaria is a major public health concern with an estimated 68 million cases and 194 000 deaths due to the disease in 2021. Nigeria has the highest burden of malaria globally, accounting for nearly 27% of the global malaria burden. The risk of transmission exists throughout the country, all year round [3]. Research on fractional order modeling of many physical phenomena is currently quite popular. Leibniz introduced the concept of the nth derivative, which is where the idea of fractional order derivatives originated. Following that, several definitions of integrals and fractional differentials were given. Three laws have been proposed in the subject of fractional calculus: the extended Mittag-Leffler law, the power law, and the exponential decay law. It was shown that the Atangana–Baleanu fractional operator is a particular instance of the Riemann–Liouville and Caputo–Fabrizio functions, and that the kernel Mittag- Leffler function is broader than power law and exponential decay function [4]. Numerous scholars have created a number of mathematical models in attempt to obtain understanding of the dynamics of malaria transmission within human populations using fractional-order modeling. In order to lower the disease's prevalence, these models have offered treatment suggestions. For instance, multiple scholars have created a number of mathematical models to get understanding of the dynamics of malaria transmission in human populations using fractional-order modeling. In order to lower the disease's prevalence, these models have offered treatment suggestions. A malaria transmission (MT) model based on Liouville–Caputo fractional-order (FO) derivatives was created by [5] to account for memory effects in the disease's spread, the model incorporates both exponential decay and power-law dynamics. Fixed-point theory was used to prove the existence and uniqueness (EU) of the solutions, which were obtained by an iterative process including Laplace transforms. To further complicate the concept, the authors investigated fractal–fractional operators with power-law and exponential decay. Numerical simulations demonstrated how particular FO derivatives (ς and ρ) affected the MT model, offering important new information for malaria prevention tactics. Fractional-order epidemiological modeling, particularly for illnesses with memory effects, is improved by this research. A fractional-order delayed Ross-Macdonald model is introduced in the work by [6] to evaluate the dynamics of malaria transmission. The model looks at how the fractional-order of the system and the Plasmodium incubation time affect the dynamic behavior of the disease. Important results show that delays in time have a large effect on the stability of the system and can even lead to Hopf bifurcations, which are transitions from stable to periodic solutions. Furthermore, the stability interval is influenced by the fractional order, emphasizing its significance in the dynamics of disease transmission. Theoretical conclusions are validated by numerical simulations, which show how these factors change the patterns of malaria transmission. This innovative method provides insights regarding malaria prevention tactics. [7] models the dynamics of HIV and malaria transmission with an emphasis on optimum control by using the Caputo fractional derivative. Using the next-generation matrix approach, the study computes the basic reproduction number and finds that early in the epidemic, greater fractional derivative orders cause the infected population to decline. The model highlights how public health education may induce memory effects, which effectively stop the spread of both illnesses. Furthermore, throughout the study, the best control techniques successfully lower the prevalence of malaria and HIV. The model's conclusions are validated using MATLAB-based numerical simulations that support the analytical findings. A brand-new five-compartmental fractal-fractional SIR-SI model is presented by [8] to investigate the transmission of malaria from people to mosquitoes. This model gives insights into illness dynamics under various control

methods and accounts for memory effects using extended Mittag-Leffler fractal-fractional derivatives. This paper investigates the stability, uniqueness, and existence of solutions using numerical simulations with a Newton polynomial. According to the findings, memory effects combined with increased antimalarial therapy greatly lowers the peak number of sick people, while spraying insecticides on mosquitoes successfully inhibits the transmission of disease across all compartments. A fractional-order mathematical model of malaria transmission is presented by [9] with an emphasis on mosquito vector phases and two categories of humans: semi-immune and non-immune. This work employs the Atangana-Baleanu fractional derivative in the Caputo sense, extending an earlier integer-order model by Ousmane Koutou and including memory effects to improve realism in portraying the dynamics of malaria. Lipschitz criteria and the fixed-point theorem were used to demonstrate the existence and uniqueness of the model. The fractional-order model, which considers the complexity of interactions between humans and mosquitoes, is more dynamic, according to numerical analysis carried out using the Generalized Euler technique. This method provides a more thorough grasp of the dynamics of malaria transmission. [10] describe a deterministic mathematical model that simulates the dynamics of malaria transmission between people and mosquitoes by utilizing the Caputo-Fabrizio (CF) fractional derivative. The model incorporates a hospitalized patient compartment and applies the next-generation matrix approach to determine equilibrium point stability conditions and calculate the fundamental reproduction number ($\mathcal{R}_0$). Sensitivity analysis of $\mathcal{R}_0$ is carried out both locally and internationally, demonstrating the resilience of the model. The Runge–Kutta fourth-order approach in MAPLE is used to do numerical simulations, demonstrating how fractional calculus might improve our comprehension of the dynamics of malaria transmission. [11] create a fractional-order mathematical model for malaria transmission in their 2021 study, considering the potential for recurrence and transient immunity. The memory effect in the dynamics of malaria is captured by the model by using the Caputo fractional operator. The authors use Lipschitz and locally limited criteria to demonstrate the uniqueness and existence of solutions. Equilibrium points undergo stability analysis, which reveals a Hopf bifurcation. To lower the number of infected hosts and vectors, two control variables are included. The model's output is verified by numerical techniques, such as the Runge-Kutta fourth-order approach and Laplace Adomian decomposition, which are backed by sensitivity and convergence studies. An ideal control strategy for a fractional-order malaria transmission dynamics model with updated parameters is examined by [12]. The model incorporates two control variables with the goal of lowering the populations of infectious humans that pose a risk to both low-risk and high-risk, using the Atangana-Beleanu fractional derivative. The authors present nonstandard finite difference techniques, which use Mittag-Leffler kernels, for simulating the model and establish essential conditions for addressing the optimum control issue. The model's effectiveness is demonstrated through the presentation of numerical simulations and comparison investigations that confirm the theoretical results. This paper explores fractional calculus inside epidemic models, which helps to malaria control measures. Using fractal-fractional operators in the Atangana-Baleanu setting, [13] offer a nonlinear mathematical model to explore the transmission dynamics of the monkeypox virus across human and rodent populations. In order to prove that a solution exists and is unique, the authors employ fixed point theorems like Banach's and Krasnoselskii's. They also examine the stability of equilibrium points and the fundamental reproduction number. Numerical methods for the model were developed using the Adams-Bashforth approach. The influence of different fractional orders and fractal dimensions on the transmission dynamics is shown by numerical simulations based on actual data, offering insights on the behavior of the illness. [14] create a fractional-order mathematical model that focuses on the propagation of human infection via mosquitoes in order to explain the Zika virus transmission process. Atangana-Baleanu-Caputo sense is used in the model's construction, and a

fractal-fractional operator with a generalized Mittag-Leffler kernel is included. The paper looks at the system's positivity and boundedness and uses fixed point theory to prove that there is a single, unique solution. Atangana-Toufik scheme numerical simulations are carried out with stability analysis taking various fractional dimensions into account. The simulations provide important insights for upcoming Zika virus management measures and confirm the theoretical results. [15] investigated various epidemiological aspects of Lassa fever viral infection using a fractional order mathematical model so as to assess the impacts of treatment and vaccination on the spread of Lassa fever transmission dynamics using a fractional order derivative with power law to enhance understanding of disease dynamics. [16] suggest a fractional-order compartmental model to investigate the dynamics of helminth infections spread via the soil. The system of nonlinear differential equations is solved in series using the Laplace Adomian Decomposition Method (LADM). The outcomes demonstrate that the series solutions produced by LADM converge to the model's precise solution. These approximations are validated by MATLAB numerical simulations. According to the study, the fractional-order model is more flexible than the classical model because it allows for alterations to the infection dynamics across different compartments by adjusting the fractional order (e.g., 0.75 to 1). A fractional-order mathematical model is created by [15] to investigate the dynamics of Lassa fever transmission and management techniques. The model starts with integer-order nonlinear differential equations that include imperfect treatment and immunization as control measures. A fractional-order derivative with a power law is used to modify the model in order to gain a better understanding of the illness transmission. The study uses the Lyapunov function to analyze the stability of the endemic equilibrium and defines requirements for the presence and uniqueness of solutions. Utilizing the fractional Adams-Bashforth-Moulton approach, numerical simulations show how changes in contact rates, treatment efficacy, and vaccination effectiveness affect the dynamics of the illness. The prevalence of Lassa fever is seen to grow with increased contact rates and worse vaccine efficiency, but it is dramatically reduced with optimal treatment and immunization tactics.

The specific objective of this paper is to apply the Fractional Adams–Bashforth–Moulton approach to get numerical solutions of the extended model.

Preliminary

Here, we provide a few fundamental definitions and findings from fractional calculus. This investigation will employ the fractional Caputo derivatives on the right and left, [17,18]. Additionally, this publication emphasizes how fractional calculus can be used to simulate real-world issues in sciences such as biomathematics and engineering, and physics.

Definition 1: Let $f \in \Lambda^{\tau}(R),$ then the left and right Caputo fractional derivative of the function f is given by

$$ {}^{d}D_{t}^{\phi} f(t) = \left({}_{t^0}D_{t}^{-(b-\phi)} \left(\frac{d}{dt} \right)^{b} f(t) \right)$$

$$ {}^{d}D_{t}^{\phi} f(t) = \frac{1}{\Gamma(b-\phi)} \int_{0}^{t} \left((t-\lambda)^{b-\phi-1} f^{b}(\lambda) \right) d\lambda \qquad (1)$$

The same way

$$ {}_{T}^{d}D_{t}^{\phi} f(t) = \left({}_{t}D_{T}^{-(b-\phi)} \left(\frac{-d}{dt} \right)^{b} f(t) \right)$$

$$ {}_{T}^{d}D_{T}^{\phi} f(t) = \frac{(-1)^{b}}{\Gamma(b-\phi)} \int_{t}^{T} \left((\lambda - t)^{b-\phi-1} f^{b}(\lambda) \right) d\lambda $$

Definition 2: The generalized Mittag-Leffler function $E_{\gamma,\alpha}(x)$ for $x \in R$ is given by

$$ E_{\gamma,\alpha}(x) = \sum_{m=0}^{\infty} \frac{x^{b}}{\Gamma(\beta b + \alpha)}, \beta, \alpha > 0 \tag{2} $$

which can also be represented as

$$ E_{\gamma,\alpha}(x) = xE_{\beta,\beta+\alpha(x)} + \frac{1}{\Gamma(\alpha)} \tag{3} $$

$$ E_{\gamma,\alpha}(x) = L\left[t^{\alpha-1} E_{\gamma,\alpha(\pm\psi t^{\gamma})} \right] = \frac{S^{\beta-\alpha}}{S^{\gamma} \pm \psi} \tag{4} $$

Proposition 1.1. Let $f \in \Lambda^{\tau}(R) \cap C(R)$ and $\gamma \in R, b-1 < \gamma < b,$
Therefore, the conditions given below holds:

1. $ {}_{t_0}^{d}D_{t}^{\phi} I^{\phi} f(t) = f(t) $
2. $ I_{t_0}^{\phi} D_{t}^{\phi} f(t) = f(t) - \sum_{k=0}^{b-k} \frac{t^{k}}{k!} f^{k}(t_0). $

1.1. Model formulation

The population is divided into eight groups in order to build the integer-order model for malaria: susceptible persons (S), People who have been exposed to malaria E_H^M, individuals infected with malaria I_H^M, People with malaria who are receiving treatment T_H^M, individuals who have recovered from malaria R. Additionally, we separated the vector population into three groups: malaria-prone vectors S_V, vectors exposed to malaria E_V and vectors infected with malaria I_V. The entire human population is represented by N_H whereas the entire vector population is symbolized by N_V.

Humans susceptible to malaria S_H^M recruits at a rate (λ). The class declines due to the rate of natural deaths and also by the proportion of individuals who become infected after contact with an infected vector β_H^M. These malaria-susceptible individuals increase at the rate at which recovered individuals become susceptible again ωR. We thus formulated the dynamics of susceptible individuals as follows:

$$ \frac{dS_H}{dt} = \Lambda_H - \left(\frac{M \beta_H^M I_V^M}{N_H} \right) S_H + \omega R - \theta_H S_H $$

Malaria exposed Humans increases due to the proportion of individuals newly infected at a rate of λ_H^M. This class decreases at the rate at which the exposed individuals become fully infected, at a rate of σE_H^M as well as the rate of natural death θ_H. This population is described by the following formulation;

$$\frac{dE_H^M}{dt} = \left(\frac{M\beta_H^M I_V^M}{N_H}\right) S_H - (\sigma + \theta_H) E_H^M,$$

Malaria Infected Humans I_H^M increases due to the progression of exposed individuals to the infected class at a rate of σE_H^M. The population decreases due to the natural death rate θ_H, due to disease-related deaths at a rate of δ, the rate at which the infected individuals are taken for treatment, at a rate of ϕI_H^M. The dynamics of this class are described as follows;

$$\frac{dI_H^M}{dt} = \sigma E_H^M - (\phi + \delta + \theta_H) I_H^M,$$

Malaria infected Humans on treatment T_H^M increases at the rate at which infected individuals are taken for treatment, at a rate of ϕI_H^M, the population decreases due to both disease-induced and natural deaths, at a rate of $\varepsilon\delta$ and θ_H respectively. The class also decreases due to recovery at a rate of αT_H^M of the treated individuals. The dynamics of this population are presented as follows;

$$\frac{dT_M}{dt} = \phi I_H^M - (\alpha + \varepsilon\delta + \theta_H) T_M,$$

Malaria recovered individuals R increases due to recovery as a result of treatment, at a rate of αT_H^M.The class ultimately decreases due to natural death at a rate of θ_H and reverts to vulnerability at a rate of ωR.This class's dynamics are expressed as;

$$\frac{dR}{dt} = \alpha T_H^M - (\omega + \theta_H) R,$$

Susceptible vectors population S_V are recruited at rate Λ_V. The class decreases at the rate at which susceptible vectors become infected after contacting infected humans, at a rate of λ_V^M and by the natural death of vectors at a rate of θ_V. The dynamics of this class are formulated as follows;

$$\frac{dS_V}{dt} = \Lambda_V - (\lambda_V^M + \theta_V) S_V$$

Where $\lambda_V^M = \frac{M\beta_V^M I_H^M}{N}$

Malaria exposed vectors class increases at the rate at which newly infected susceptible individuals progress to the exposed class, at a rate of λ_V^M, The class decreases at the rate at which exposed vectors become fully infected, at a rate of γ_V, as well as the rate of natural death θ_V. The following is a formulation of the class dynamics.

$$\frac{dE_V}{dt} = \lambda_V^M S_V - (\gamma_V + \theta_V) E_V$$

Malaria infected vectors I_V The class increases due to the progression of exposed individuals becoming fully infectious, at a rate of γ_V . This class decreases due to natural recovery at a rate of θ_V .The dynamics of this class are formulated as follows:

$$\frac{dI_V}{dt} = E_V\gamma_V - \theta_V I_V$$

.

The force of infection associated with this human population is expressed as:

$$\lambda_H^M = \frac{M\beta_H^M I_V^M}{N_H}$$

However, that related to the population of vectors is provided by

$$\lambda_V^M = \frac{M\beta_V^M I_H^M}{N}$$

The following represents the mathematical model that aligns with our presumptions and the previous description:

$$\begin{aligned}
&\tfrac{dS_H}{dt} = \Lambda_H - \lambda_H^M S_H + \omega R - \theta_H S_H,\\
&\tfrac{dE_H^M}{dt} = \lambda_H^M S_H - (\sigma + \theta_H)E_H^M,\\
&\tfrac{dI_H^M}{dt} = \sigma E_H^M - (\phi + \delta + \theta_H)I_H^M,\\
&\tfrac{dT_M}{dt} = \phi I_H^M - (\alpha + \varepsilon\delta + \theta_H)T_M,\\
&\tfrac{dR}{dt} = \alpha T_H^M - (\omega + \theta_H)R,\\
&\frac{dS_V}{dt} = \Lambda_V - (\lambda_V^M + \theta_V)S_V\\
&\frac{dE_V}{dt} = \lambda_V^M S_V - (\gamma_V + \theta_V)E_V\\
&\frac{dI_V}{dt} = E_V\gamma_V - \theta_V I_V
\end{aligned} \qquad (5)$$

.

2.0 Fractional malaria mathematical model

In this section, we use the Caputo fractional derivative operator to expand the integer model of malaria shown in Eq. (5). Since the output of the fractional order model can be changed to produce different answers, the new model that uses the Caputo fractional derivative operator has a higher degree of freedom than the classical model that is shown in Eq. (5). Thus, the following is how the fractional malaria approach is presented:

The flow diagram for the model that matches the assumption we made is displayed in

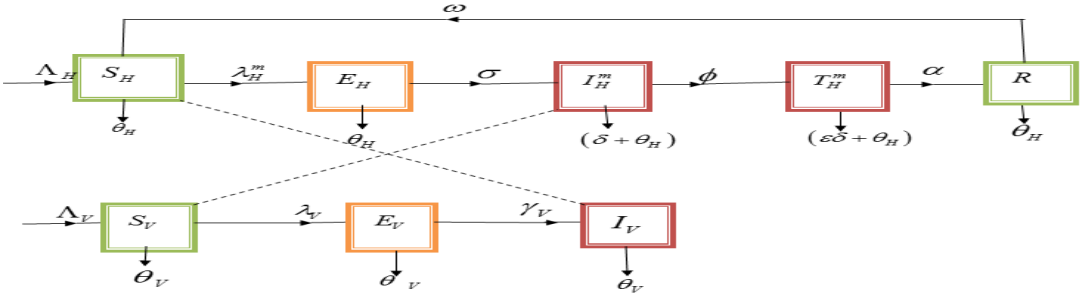

Fig 1: Schematic diagram depicting the transmission dynamics involving Malaria

3.0 Fractional malaria mathematical model

$$
\begin{aligned}
{}^{d}D_t^{\phi} S_H &= \Lambda_H - \lambda_H^M S_H + \omega R - \theta_H S_H,\\
{}^{d}D_t^{\phi} E_H^M &= \lambda_H^M S_H - (\sigma + \theta_H) E_H^M,\\
{}^{d}D_t^{\phi} I_H^M &= \sigma E_H^M - (\phi + \delta + \theta_H) I_H^M,\\
{}^{d}D_t^{\phi} T_H^M &= \phi I_H^M - (\alpha + \varepsilon\delta + \theta_H) T_H^M,\\
{}^{d}D_t^{\phi} R &= \alpha T_H^M - (\omega + \theta_H) R,\\
{}^{d}D_t^{\phi} S_V &= \Lambda_V - (\lambda_V^M + \theta_V) S_V,\\
{}^{d}D_t^{\phi} E_V &= \lambda_V^M S_V - (\gamma_V + \theta_V) E_V,\\
{}^{d}D_t^{\phi} I_V &= E_V \gamma_V - \theta_V I_V.
\end{aligned}
\tag{6}
$$

Where

$$L_1 = (\sigma + \theta_H),\ L_2 = (\phi + \delta + \theta_H),\ L_3 = (\alpha + \varepsilon\delta + \theta_H),\ L_4 = (\omega + \theta_H),\ L_5 = (\gamma_V + \theta_V).$$

Subject to the positive initial conditions

$$
\begin{aligned}
&S_H(0) = S_{H0}, E_H^M(0) = E_{H0}^M, I_H^M(0) = I_{H0}^M, T_H^M(0) = T_{H0}^M, R(0) = R_0, S_V(0) = S_{V0}(0),\\
&E_V(0) = E_{V0}(0), I_V(0) = I_{V0}(0).
\end{aligned}
\tag{7}
$$

3.0 The basic reproduction number (R0) and model equilibrium points

The model (5)'s disease-free equilibrium point can be written as follows:

$$MDFEP = \left\{S_H^*, E_H^{M*}, I_H^{M*}, T_H^*, R_H^*, S_V^*, E_V^*, I_V^*\right\} = \left\{\frac{\Lambda_H}{\theta_H}, 0, 0, 0, 0, \frac{\Lambda_V}{\theta_V}, 0, 0\right\} \tag{7}$$

We utilize the technique developed by [30] and obtained the basic reproduction number as:

$$R_0^M = \frac{\sqrt{L_1 L_2 L_5 \Lambda_H \beta_V \theta_H \Lambda_V \sigma \beta_H \gamma_V M}}{\theta_V L_1 L_2 L_5 \Lambda_H}$$

Since $L_1 = (\sigma + \theta_H),\ L_2 = (\phi + \delta + \theta_H),\ L_3 = (\alpha + \varepsilon\delta + \theta_H),\ L_4 = (\omega + \theta_H),\ L_5 = (\gamma_V + \theta_V).$

$$R_0^M = \frac{\sqrt{(\sigma + \theta_H)(\phi + \delta + \theta_H)(\gamma_V + \theta_V)\Lambda_H \beta_V \theta_H \Lambda_V \sigma \beta_H \gamma_V M}}{\theta_V (\sigma + \theta_H)(\phi + \delta + \theta_H)(\gamma_V + \theta_V)\Lambda_H} \tag{8}$$

4. Fractional order model numerical results

We numerically solved the fractional order Malaria model using the generalized fractional Adams Bashforth–Moulton approach described in [19]; the values of the Model Parameters employed are shown in Table 1, where various fractional order (γ) values are taken into consideration and simulated.

4.1. Implementation of fractional Adams–Bashforth–Moulton method

This work uses the methodology outlined by [20], [21], and [22]. We used the fractional Adam–Bashforth–Moulton approach to find an approximate solution of the fractional malaria model shown in (6). Now shows the fractional model (6) as follows:

$$
\begin{aligned}
&{}^{d}D_t^{\phi} G(t) = N(t, G(t)),\ 0 < t < \psi\\
&G^{(n)}(0) = G_0^{(n)},\ n = 1, 0, \ldots, G, G = [\phi].
\end{aligned}
\tag{9}
$$

Where $G = \left(S_H^*, E_H^{M^*}, I_H^{M*}, T_H^{M^*}, R_H^*, S_V^*, E_V^*, I_V^*\right) \in R_+^8$ and $Q(t, G(t))$ is a continuous, real-valued function. Therefore, the fractional integral idea can be used to represent Eq. (9) as follows:

$$G(t) = \sum_{n=0}^{G-1} G_0^{(n)} \frac{t^n}{n!} + \frac{1}{\Gamma(\phi)} \int_0^t (t - y)^{\phi - 1} R(y, G(y))\, dy \tag{10}$$

Following [6] process, we permitted the step size $q = \frac{\psi}{N}, N \in \mathrm{N}$ utilizing a consistent grid on $[0, \psi]$. Where $t_c = cr, c = 0,1,1,...N.$ Consequently, the following is an approximate representation of the malaria fractional order model displayed in (6):

$$
\begin{aligned}
S_{H\,k+1}(t) &= S_{H0} + \frac{q^{\phi}}{\Gamma(\phi+2)}\left\{\Lambda_H - \left(M\beta_H^M I_V^M\right)\frac{S_H^n}{N_H^n} + \omega R_H^n - \theta_H S_H^n\right\} \\
&+ \frac{q^{\phi}}{\Gamma(\phi+2)}\sum_{v=0}^{k} dy, k+1\left\{\Lambda_H - \left(M\beta_H^M I_V^M\right)\frac{S_H^n}{N_H^n} + \omega R_H^n - \theta_H S_H^n\right\} \\
E_{H\,k+1}^M(t) &= E_{H0}^M + \frac{q^{\phi}}{\Gamma(\phi+2)}\left\{\left(\frac{M\beta_H^M I_V^M}{N_H}\right)S_H - L_1 E_H^M\right\} \\
&+ \frac{q^{\phi}}{\Gamma(\phi+2)}\sum_{v=0}^{k} dy, k+1\left\{\left(\frac{M\beta_H^M I_V^M}{N_H}\right)S_H - L_1 E_H^M\right\} \\
I_{H\,k+1}^M(t) &= I_{H0}^M + \frac{q^{\phi}}{\Gamma(\phi+2)}\left\{\sigma E_H^M - L_2 I_H^M\right\} \\
&+ \frac{q^{\phi}}{\Gamma(\phi+2)}\sum_{v=0}^{k} dy, k+1\left\{\sigma E_H^M - L_2 I_H^M\right\} \\
T_{H\,k+1}^M(t) &= T_{H0}^M + \frac{q^{\phi}}{\Gamma(\phi+2)}\left\{\phi I_H^M - L_3 T_M\right\} \\
&+ \frac{q^{\phi}}{\Gamma(\phi+2)}\sum_{v=0}^{k} dy, k+1\left\{\phi I_H^M - L_3 T_M\right\} \\
R_{H\,k+1}(t) &= R_{H0} + \frac{q^{\phi}}{\Gamma(\phi+2)}\left\{\alpha T_H^M - L_4 R_H\right\} \\
&+ \frac{q^{\phi}}{\Gamma(\phi+2)}\sum_{v=0}^{k} dy, k+1\left\{\alpha T_H^M - L_4 R_H\right\} \\
S_{V\,k+1}(t) &= S_{V0} + \frac{q^{\phi}}{\Gamma(\phi+2)}\left\{\Lambda_V - L_5 S_V\right\} \\
&+ \frac{q^{\phi}}{\Gamma(\phi+2)}\sum_{v=0}^{k} dy, k+1\left\{\Lambda_V - L_5 S_V\right\} \\
E_{V\,k+1}(t) &= E_{V0} + \frac{q^{\phi}}{\Gamma(\phi+2)}\left\{\lambda_V^M S_V - L_6 E_V\right\} \\
&+ \frac{q^{\phi}}{\Gamma(\phi+2)}\sum_{v=0}^{k} dy, k+1\left\{\lambda_V^M S_V - L_6 E_V\right\} \\
I_{V\,k+1}(t) &= I_{V0} + \frac{q^{\phi}}{\Gamma(\phi+2)}\left\{E_V\gamma_V - \theta_V I_V\right\} \\
&+ \frac{q^{\phi}}{\Gamma(\phi+2)}\sum_{v=0}^{k} dy, k+1\left\{E_V\gamma_V - \theta_V I_V\right\}
\end{aligned}
\tag{11}
$$

Where;

$$
\begin{aligned}
S_{Hk+1}^n(t) &= S_{H0} + \frac{1}{\Gamma(\phi)}\sum_{v=0}^{k} f_{v,k+1}\left\{\Lambda_H - \left(M\beta_H^M I_V^M\right)\frac{S_H^n}{N_H^n} + \omega R_H^n - \theta_H S_H^n\right\}, \\
E_{HK+1}^M(t) &= E_{H0}^M + \frac{1}{\Gamma(\phi)}\sum_{v=0}^{k} f_{v,k+1}\left\{\left(\frac{M\beta_H^M I_V^M}{N_H}\right)S_H - L_1 E_H^M\right\}, \\
I_{HK+1}^M(t) &= I_{H0}^M + \frac{1}{\Gamma(\phi)}\sum_{v=0}^{k} f_{v,k+1}\left\{\sigma E_H^M - L_2 I_H^M\right\},
\end{aligned}
$$

$$
\begin{aligned}
T^{M}_{HK+1}(t) &= T^{M}_{H0} + \frac{1}{\Gamma(\phi)}\sum_{y=0}^{k} f_{y,k+1}\left\{\phi I^{M}_{H} - L_3 T_M\right\},\\
R_{HK+1}(t) &= R_{H0} + \frac{1}{\Gamma(\phi)}\sum_{y=0}^{k} f_{y,k+1}\left\{\alpha T^{M}_{H} - L_4 R_H\right\},\\
S_{VK+1}(t) &= S_{V0} + \frac{1}{\Gamma(\phi)}\sum_{y=0}^{k} f_{y,k+1}\left\{\Lambda_V - L_5 S_V\right\},\\
E_{VK+1}(t) &= E_{V0} + \frac{1}{\Gamma(\phi)}\sum_{y=0}^{k} f_{y,k+1}\left\{\lambda^{M}_{V} S_V - L_6 E_V\right\}\\
I_{VK+1}(t) &= I_{V0} + \frac{1}{\Gamma(\phi)}\sum_{y=0}^{k} f_{y,k+1}\left\{E_V\gamma_V - \theta_V I_V\right\}.
\end{aligned}
\qquad (12)
$$

From (11) and (12) we obtained;

$$
dy_{,K+1} = K^{\phi+1} - (k-\phi)(k+\phi)^{\phi},\ y=0
$$

$$
(k-y+2)^{\phi+1} + (k-\phi)^{\phi+1} - 2(k-y+1)^{\phi+1},\ 1 \le y \le k
$$

$$
1,\ y = k+1
$$

And

$$
f_{y,k+1} = \frac{q^{\phi}}{\phi}\left[(k-y+1)^{\phi}(k-y)^{\phi}\right],\ 0 \le y \le k.
$$

Table 1: Values of model parameters used for simulation

Parameters	Description	Value	Source
Λ	Rate of susceptible persons recruited**.**	0.00011	[28]
θ_h	Rate of human natural death	0.00004	[27]
θ_V	Rate of vector natural death	0.04	[26]
σ	Rate at which a class becomes infected	0.01	Fitted
β^{m}_{H}	Human contact rate	0.8962	Fitted
β_V	vector contact rate	0.09	Fitted
δ_m	Malaria-related mortality rate in humans.	0.0003454	[31]
α	Rate of recuperation from a malaria infection	0.1	Fitted
Λ_V	Recruitment rate within the vector population.	0.071	[25]
γ_V	Rate at which vectors that have been exposed develop infection.	0.056	[28]
ω	The rate at which people recuperate from malaria and turn susceptible.	0.1	Fitted
ε	Modification parameter	0.11	Estimated

Sources:https://www.afro.who.int/sites/default/files/2023-08/WEB_7784%20WMR%20-%20Nigeria%202022_2408.pdf

4.2. Importance of using the fractional Adam-Bashforth Moulton method in obtaining the numerical solutions of the model

• The fractional Adam–Bashforth Moulton method delivers high-order accuracy with just one extra function evaluation per step.

• The Adam–Bashforth Moulton method is frequently utilized in packaged ODE solvers and provides automatic error control.

• This approach is a helpful tool for numerical solutions of partial and fractional order differential equations and has potential applications in a number of sectors, including engineering, chemistry, and medicine.

4.3 Numerical Simulation

This section displays the graphs and accompanying interpretations from our numerical simulation.

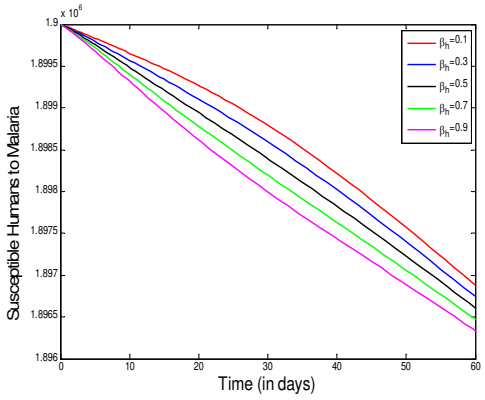

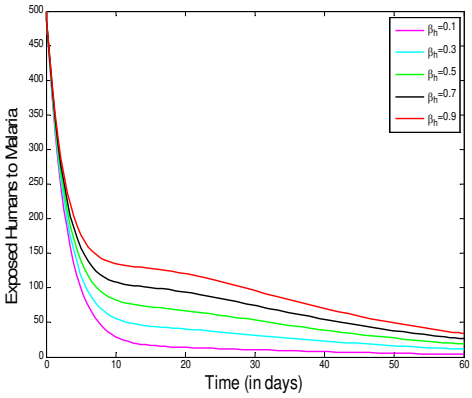

Fig. 2(*a*): Effect of varying β_H^M on Human Susceptible to Malaria

2(b): Effect of varying β_H^M on HumansExposed to malaria

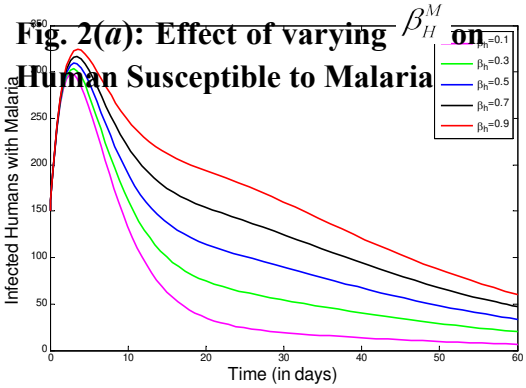

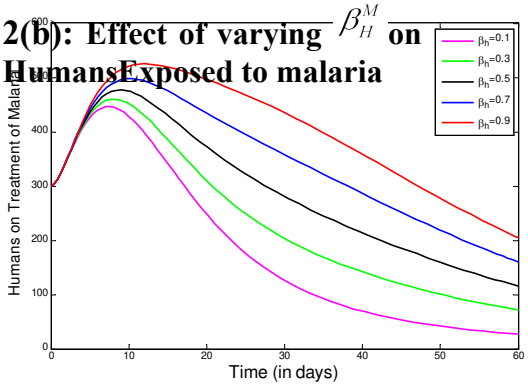

3(a): Effect of varying β_H^M on Human Infected with Malaria

3(b): Effect of varying β_H^M on Treated humans due to malaria

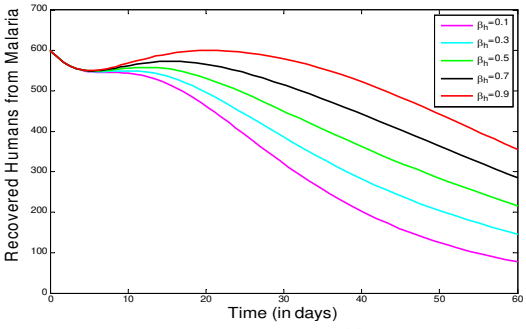

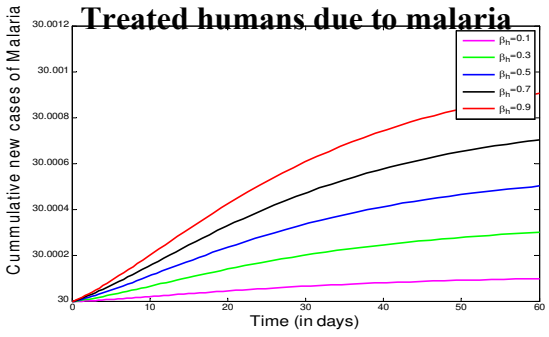

4(a): Effect of varying β_H^M on Recovered humans from malaria

Fig.4(b): Effect of varying β_H^M on cumulative new cases of Malaria

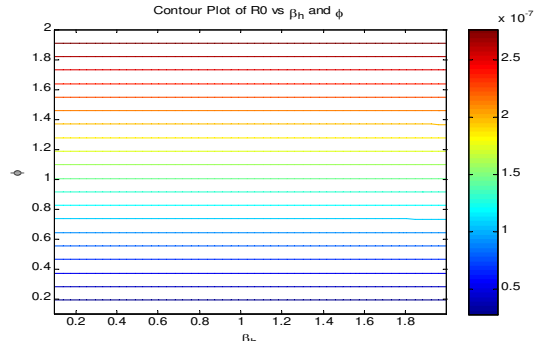

5(a) contour plot showing the impact of ϕ and β_H on R_0

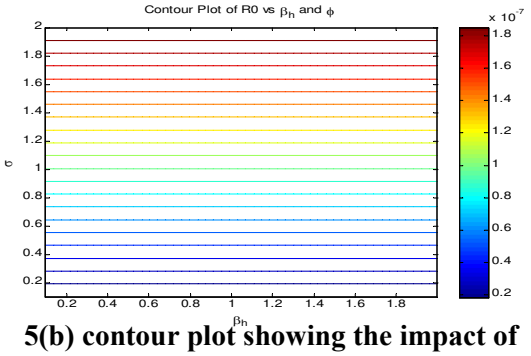

5(b) contour plot showing the impact of σ and β_H on R_0

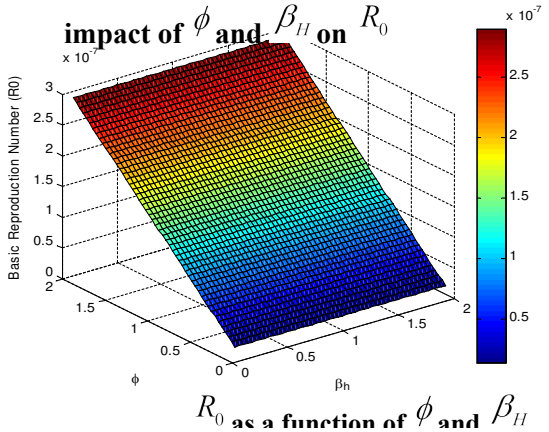

R_0 as a function of ϕ and β_H

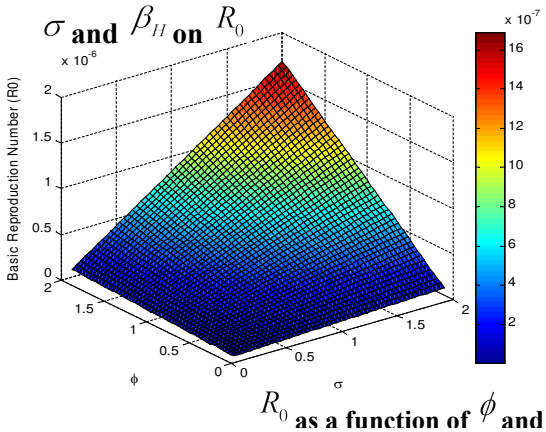

R_0 as a function of ϕ and σ

Figure (2a) shows how changing the fractional order derivative over time affects the vulnerable human population. The plot clearly shows that when the sensitive human population rises, the population falls. This decline is explained by the application of treatment strategies, which lower the number of people at risk for contracting the illness. We saw a similar pattern in Figure (2b): a decline in the sensitive person class. With treatment accessible as an intervention approach, the number of persons at risk of catching malaria will steadily decrease, allowing the disease's overall impact on the human population to be greatly decreased, as demonstrated by this fall in the exposed class.

The graph in Figure (3a) illustrates how the infectiousness of malaria in the human population initially led to a surge in the number of members of the infected class by drawing in members from the exposed class. But ultimately, the effect of treatment on the general populace results in a sharp drop in the number of afflicted individuals. This illustrates how the use of treatment techniques can greatly lower the burden of malaria on the human population. In contrast to the graph's behavior in Figure (3b), the number of individuals in the treatment class increases as more people from the malaria-infected class join it. Later, the treatment graph for patients with malaria shows a consistent decline.

Figure (4a) illustrates how an effective treatment intervention for human malaria subsequently results in a notable increase in the population of individuals who have recovered from malaria. We were able to infer from the graph in figure (4b) that a greater contact rate between susceptible individuals and infected vectors was the reason for an increase in the total number of new cases of malaria. This calls for acting to reduce human-mosquito contact, such as mandating the use of treated mosquito nets in homes and even at treatment centers.

The contour plot is shown in the graph in Fig. (5a). of ϕ and β_H concerning R_0. Also, it is clear by looking at the numerical streams in the graph that the highest value R_0 can obtained by

adjusting these parameters is 0.6, which is less than unity (1). This finding implies that increasing these factors wouldn't result in a substantial population-wide malaria outbreak. Fig. (5b) illustrates the contour plot of σ and β_H concerning R_0. It is clear by looking at the numerical streams in the graph that the highest value that R_0 can obtained by adjusting these parameters is 0.6, which is less than unity (1). This finding implies that increasing these factors wouldn't result in a substantial population-wide malaria outbreak.

Figure (6a) shows the basic reproduction number R_0 reaches a peak below one (1) as the values of ϕ and β_H increase. This suggests that raising these metrics will eventually lessen the population's exposure to malaria. On the other hand, if suitable steps are not taken, ϕ and σ can make the incidence of malaria worse. This is demonstrated by their impact on R_0, as shown in Fig. (6b), leading it to peak above one (1).

Conclusion

The mathematical model for the dynamics of malaria transmission and control in the sense of Caputo is presented in this work. Given the importance of fractional modeling. We solved the fractional model numerically using the fractional Adams–Bashforth–Moulton method. Considering different fractional orders of the Caputo operator and model parameter values, the generated simulations graphically represented the disease's incidence impact. Additionally, we ran simulations by changing variables like the contact rate between susceptible and infected people and the contact rate for infected people. The results showed that increasing the treatment approach will successfully reduce the incidence of malaria in the general population. This approach can be used in future work to solve the problems examined in [23] Novel trial functions and rogue waves of generalized breaking soliton equations via bilinear neural network method, which creates a general symbolic computing path for the analytic solution of Non-linear partial differential equations.

References

[1] World Health Organization. (2023). Malaria. Retrieved from https://www.who.int/news-room/fact-sheets/detail/malaria.

[2] Centers for Disease Control and Prevention. (2023). World Malaria Day 2023. Accessible at: https://www.cdc.gov/malaria/index.html

[3] World Health Organization. (2022). *World malaria report 2022*. https://www.afro.who.int/countries/nigeria/publication/report-malaria-nigeria-2022

[4] Ali, A., Khan, M. Y., Sinan, M., Allehiany, F. M., Mahmoud, E. E., Abdel-Aty, A., & Ali, G. (2021). Theoretical and numerical analysis of novel COVID-19 via fractional order mathematical model. *Results in Physics, 20*, 103676. https://doi.org/10.1016/j.rinp.2020.103676.

[5] Gómez-Aguilar, J. F., Cordova, T., Abdeljawad, T., Khan, A., & Khan, H. (2020). Analysis of fractal-fractional malaria transmission model. *Fractals, 28*. https://doi.org/10.1142/S0218348X20400411

[6] Cui, X., Xue, D., & Li, T. (2021). Fractional-order delayed Ross-Macdonald model for malaria transmission. https://doi.org/10.21203/rs.3.rs-357785/v1

[7] Cheneke, K. (2023). Fractional derivative model for analysis of HIV and malaria transmission dynamics. *Discrete Dynamics in Nature and Society, 2023*, 1–17. https://doi.org/10.1155/2023/5894459

[8] Rezapour, S., Etemad, S., Asamoah, J., Ahmad, H., & Nonlaopon, K. (2022). A mathematical approach for studying the fractal-fractional hybrid Mittag-Leffler model of malaria under some control factors. *AIMS Mathematics, 8*, 3120–3162. https://doi.org/10.3934/math.2023161

[9] Pawar, D. D., Patil, W. D., & Raut, D. K. (2021). Analysis of malaria dynamics using its fractional order mathematical model. *Journal of Applied Mathematics & Informatics, 39*(1–2), 197–214.

https://doi.org/10.14317/jami.2021.197
[10] Alqahtani, A. S., Ramzan, S., Zanib, S. A., Nazir, A., Masood, K., & Malik, M. Y. (2024). Mathematical modeling and simulation for malaria disease transmission using the CF fractional derivative. *Alexandria Engineering Journal, 101*, 193–204. https://doi.org/10.1016/j.aej.2024.05.055
[11] Rehman, A. ul, Singh, R., Abdeljawad, T., Okyere, E., & Guran, L. (2021). Modeling, analysis, and numerical solution to malaria fractional model with temporary immunity and relapse. *Advances in Difference Equations, 2021*(390). https://doi.org/10.1186/s13662-021-03532-4
[12] Sweilam, N. H., AL-Mekhlafi, S. M., & Albalawi, A. O. (2020). Optimal control for a fractional order malaria transmission dynamics mathematical model. *Alexandria Engineering Journal*, Elsevier B.V. http://creativecommons.org/licenses/by-nc-nd/4.0/
[13] Sudsutad, W., Thaiprayoon, C., Kongson, J., & Sae-dan, W. (2024). A mathematical model for fractal-fractional monkeypox disease and its application to real data. *AIMS Mathematics, 9*(4), 8516–8563. https://doi.org/10.3934/math.2024414
[14] Farman, M., Akgül, A., Askar, S., Botmart, T., Ahmad, A., & Ahmad, H. (2022). Modeling and analysis of fractional order Zika model. *AIMS Mathematics, 7*(3), 3912–3938. https://doi.org/10.3934/math.2022216
[15] Atokolo, W., Aja, R., Omale, D., Ahman, Q., Acheneje, G., & Amos, J. (2024). Fractional mathematical model for the transmission dynamics and control of Lassa fever. *Franklin Open, 7*, 2773–1863. https://doi.org/10.1016/j.fraope.2024.100110.
[16] Omede, B., Israel, M., Mustapha, M., Amos, J., Atokolo, W., & Oguntolu, F. (2024). Approximate solution to fractional order soil-transmitted helminth infection model using Laplace Adomian decomposition method, 16–40. https://doi.org/10.5281/zenodo.11630908
[17] Milici, C., Draganescu, G., & Machado, J. T. (2018). Introduction to fractional differential equations. Springer.
[18] Podlubny, I. (1998). Fractional differential equations, an introduction to fractional derivatives. In *Fractional Differential Equations*, Methods of their Solutions and Some of their Applications. Elsevier.
[19] Chen, S. B., Rajaee, F., Yousefpour, A., Alcaraz, R., Chu, Y. M., Gómez-Aguilar, J. F., & Jahanshahi, H. (2021). Antiretroviral therapy of HIV infection using a novel optimal type-2 fuzzy control strategy. *Alexandria engineering journal*, *60*(1), 1545-1555.
[20] Diethelm, K. (1999). The FracPECE subroutine for the numerical solution of differential equations of fractional order.
[21] Liu, B., Farid, S., Ullah, S., Altanji, M., Nawaz, R., & Teklu, S. W. (2023). Mathematical assessment of monkeypox disease with the impact of vaccination using a fractional epidemiological modeling approach. *Scientific Reports*. https://doi.org/10.1038/541598-023-40745
[22] Baskonus, H. M., & Bulut, H. (2015). On the numerical solutions of some fractional ordinary differential equations by fractional Adams Bashforth-Moulton Method. *Open Math, 13*, 1.
[23] Zhang, R. F., Li, M.-C., Gan, J. Y., Li, Q., & Lan, Z.-Z. (2022). Novel trial functions and rogue waves of generalized breaking soliton equation via bilinear neural network method. *Chaos, Solitons & Fractals, 154*(C).
[24] Atokolo W a, Remigius Aja .O. , Omale .D., Paul .R. V. ,Amos . J.,Ocha S. O., (2023) Mathematical modeling of the spread of vector borne diseases with influence of vertical transmission and preventive strategies FUDMA Journal of sciences: Vol. 7 No. 6, December (Special Issue), pp 75 -91 DOI: https://doi.org/10.33003/fjs-2023-0706-2174
[25] Afolabi, M. O., Adebiyi, A., Cano, J., Sartorius, B., Greenwood, B., Johnson, O., & Wariri, O. (2022). Prevalence and distribution pattern of malaria and soil-transmitted helminth co-endemicity in sub-Saharan Africa, 2000–2018: A geospatial analysis. *PLoS Neglected Tropical Diseases, 16*(9), e0010321.
[26] Castillo-Chavez, C., & Song, B. (2004). Dynamics models of tuberculosis and their applications. *Math. Biosci, 2*, 361–404.
[27] Nayeem, J., & Sultana, I. (2019). Transmission dynamics of tuberculosis at the population level: A dynamical model. *Chaos, Solitons & Fractals, 119*, 133–142.
[28] Ojo, M. M., Olumuyiwa, P., Goufo, E. F., & Nisar, K. S. (2023). A mathematical model for the co-dynamics of COVID-19 and tuberculosis. *Mathematics and Computers in Simulation, 207*, 499–520. https://doi.org/10.1016/j.matcom.2023.01.014

[29] Pinto, C. M., & Machado, J. T. (2013). Fractional model for malaria transmission under control strategies. *Computers & Mathematics with Applications, 66*(5), 908–916.
[30] Vanden Driessche, P., & Watmough, J. (2002). Reproduction numbers and sub-threshold endemic equilibria for compartmental models of disease transmission. *Math. Biosci, 180*(1–2), 29–48.
[31] Zhao, S., Stone, L., Gao, D., & He, D. (2018). Modelling the large-scale yellow fever outbreak in Luanda, Angola, and the impact of vaccination. *PLoS Neglected Tropical Diseases, 12*(1), e0006158. https://doi.org/10.1371/journal.pntd.0006158.